Available online at www.sciencedirect.com
ScienceDirect
ELSEVIER
JOURNAL OF RARE EARTHS, Vol. 32, No. 6, Jun. 2014, P. 508
JOURNAL OF RARE EARTHS
www.re-journal.com/en/

# Synthesis and luminescence properties of $CeF_3$:$Tb^{3+}$ nanodisks via ultrasound assisted ionic liquid method

LIU Sanxi (刘三喜)[1], HUI Yu (惠 宇)[2], ZHU Ling (朱 玲)[1,*], FAN Xizhi (范习之)[2], ZOU Binglin (邹兵林)[2], CAO Xueqiang (曹学强)[2,*]

*(1. Hunan Provincial Key Laboratory of Materials Protection for Electric Power and Transportation, School of Chemistry and Biological Engineering, Changsha University of Science and Technology, Changsha 410114, China; 2. State Key Laboratory of Rare Earth Resource Utilization, Changchun Institute of Applied Chemistry, Chinese Academy of Sciences, Changchun 130022, China)*

Received 23 October 2013; revised 7 March 2014

**Abstract:** $CeF_3$ and $CeF_3$:$Tb^{3+}$ nanocrystals were successfully synthesized by the ultrasound assisted ionic liquid (IL) method at room temperature. X-ray diffraction (XRD), scanning electron microscopy (SEM), transmission electron microscopy (TEM), selected area electron diffraction (SAED), high-resolution transmission electron micrographs (HRTEM) and photoluminescence (PL) spectra were employed to characterize the nanocrystals. The results of XRD indicated that the obtained samples crystallized well with a hexagonal phase crystal structure. SEM and TEM images demonstrated that the obtained $CeF_3$:$Tb^{3+}$ nanocrystals had a discoid shape in the presence of ultrasound and IL, whereas only granular nanoparticles were obtained by magnetic stirring. The possible formation mechanisms of the crystal growth were proposed. The PL spectra of the $CeF_3$:$Tb^{3+}$ nanodisks exhibited a strong green emission when excited at 254 nm. Furthermore, the photoluminescence intensity of $CeF_3$:$Tb^{3+}$ of the discoid particles was largely improved compared with that of the granular nanoparticles.

**Keywords:** ultrasound; ionic liquid; $CeF_3$:$Tb^{3+}$ nanocrystals; luminescence; rare earths

Rare-earth-based nanomaterials have attracted extensive research interests because of their promising applications in optical amplifiers[1], biological applications[2–5], light emitting devices (LEDs)[6], photocatalysis[7], and so forth. Among various rare-earth-based nanomaterials, $CeF_3$ has received considerable attention for several applications. Studies indicate that $CeF_3$ can be used as solid lubricant[8] and scintillator[9], as well as an important fluorescent host material owing to its low vibration energies and the subsequent minimization of the quenching of the excited state of the rare-earth ions[10]. It is well known that the shape and size of rare-earth fluoride nanocrystals have a significant effect on their chemical and physical properties. Therefore, the synthesis of nanocrystals with controllable morphology and uniform sizes is also a subject of interest. It has been found that two dimension (2D) shaped nanocrystals with large surface area and high aspect ratio have potential applications in information storage, whisper gallery mode lasers, transducer, light emitter, catalyst, and sensor[11,12]. Up to now, several approaches have been employed to synthesize discoid shapes $CeF_3$:$Tb^{3+}$ nanocrystals. For instance, Guo[13] has synthesized $CeF_3$:$Tb^{3+}$ nanodiskettes via a hydrothermal microemulsion method with bis(2-ethylhexyl)sulfosuccinate (AOT) as the template to control the sizes and shapes of nanocrystals. Zhu et al.[14] reported an ultrasound-assisted route to fabricate disk shaped $CeF_3$:$Tb^{3+}$ nanocrystals using toxic $KBF_4$ as the fluoride source. However, these synthesis approaches require either high temperature, time consumption and template or toxic fluoride reagents, which would limit their universal technical applications. Therefore, exploring a more facile, template-free and environmentally benign approach for the synthesis of 2D $CeF_3$:$Tb^{3+}$ nanostructures still is a challenge.

Currently, ionic liquids (ILs) have garnered a tremendous amount of attention owing to their fascinating properties such as high melting point, negligible vapor pressure, reasonable thermal stability, good dissolving ability, high polarity, etc.[15,16]. Thus, ILs are regarded as "green solvents" to replace traditional volatile and toxic organic solvents for long-lasting development of human society. Herein, we reported a facile, simple, low-cost and environmentally friendly ultrasound assisted ionic liquid method, which was used to synthesize 2D $CeF_3$ and $CeF_3$:$Tb^{3+}$ nanodisks. In addition, the morphology, struc-

**Foundation item:** Project supported by National Natural Science Foundation of China (21001017, 21171160, 21376031), the Lotus Scholars Program of Hunan, the Natural Science Foundation of Hunan Province (13JJ3068), and Hunan Provincial Key Laboratory of Materials Protection for Electric Power and Transportation (2014CL03, 2014CL05)

* **Corresponding authors:** ZHU Ling, CAO Xueqiang (**E-mail:** zhulingster@gmail.com, xcao@ciac.ac.cn; **Tel.:** +86-731-85258733, +86-431-85262285)

**DOI:** 10.1016/S1002-0721(14)60100-9

ture and luminescent properties of $CeF_3$ and $CeF_3$:$Tb^{3+}$ nanodisks were investigated. The possible formation mechanisms of the samples were discussed in the paper. In this system, IL 1-butyl-3-methylimidazolium tetrafluoroborate ([BMIM][$BF_4$]) acted as fluorine source, template and co-solvent.

## 1 Experimental

### 1.1 Materials

$Ce(NO_3)_3{\cdot}6H_2O$ (99%, Sinopharm Chemical Reagent Co., Ltd.), [BMIM][$BF_4$] (99%, Lanzhou Institute of Chemical Physics CAS, China) and $Tb_4O_7$ (99.99%, Shanghai Chemical Reagent) were used as starting materials. All the reagents were of analytical grade.

### 1.2 Synthesis of $CeF_3$:$Tb^{3+}$ and $CeF_3$ nanocrystals

Preparation of $CeF_3$:$Tb^{3+}$ (10 mol.% $Tb^{3+}$) nanodisks: in a typical synthesis, appropriate amounts of $Tb_4O_7$ was first dissolved in 10% nitric acid, and then mixed with $Ce(NO_3)_3$ (18 mL, 3.60 mmol) aqueous solution in a 100 mL polytetrafluoroethylene beaker under magnetic stirring for 5 min. Subsequently, 2 mL ionic liquid was added dropwise into the above mixed solution under magnetic stirring for another 5 min to form a homogeneous solution. Finally, the above homogeneous solution was exposed to ultrasound irradiation in ambient air for 2 h. Ultrasonic waves were emitted from a titanium horn, which was directly immersed in the reaction solution. The total acoustic power injected into the solution was 238 W. After irradiation, the white precipitate was collected by centrifugation at a speed of 9000 r/min for 4 min, washed with deionized water and ethanol twice in sequence to remove residual impurities, and then dried at 70 °C for 12 h. For comparison, a sample of $CeF_3$:$Tb^{3+}$ nanoparticles were also synthesized via vigorous magnetic stirring under the same condition. The $CeF_3$ nanodisks were prepared in the similar way, except that 20 mL 0.2 mol/L $Ce(NO_3)_3$ aqueous solution was used instead of the mixed solution of $Ce(NO_3)_3$ and $Tb(NO_3)_3$.

### 1.3 Characterization

X-ray diffraction diffraction (XRD) was carried out on a Bruvker D8-advance X-ray diffractometer equipped with Cu Kα radiation ($\lambda$=0.154056 nm). Scanning electron microscope (SEM) images were obtained on a Hitachi S- 4800 SEM operated at an accelerating voltage of 10 kV. Transmission electron microscope (TEM) and high- resolution transmission electron microscope (HRTEM) images were performed with a Philips TF-F20 transmission electron microscope with acceleration voltage of 200 kV. The room temperature photoluminescence spectra (PL) of the samples were recorded on a Hitachi F-7000 spectrophotometer equipped with a 150 W xenon lamp as the excitation source.

## 2 Results and discussion

### 2.1 Structural properties

The phase structure of the as-synthesized products was carried out using powder XRD. Fig. 1 shows XRD patterns of $CeF_3$ ultrasonic irradiation for 2 h (1), $CeF_3$:$Tb^{3+}$ stirring for 2 h (2), $CeF_3$:$Tb^{3+}$ ultrasonic irradiation for 2 h (3), as well as the calculated line pattern for $CeF_3$. The lattice parameters of the undoped $CeF_3$ (1) were calculated to be $a$=0.71545 nm, $c$=0.72073 nm, which closely match the standard pattern of $CeF_3$ (JCPDS No. 89-1933). No peaks of other phases or impurities could be observed, suggesting the high purity of as-obtained samples. The XRD patterns of the $Tb^{3+}$ ions doped $CeF_3$ (2, 3) are similar to the undoped $CeF_3$ and no impurity lines are observed, showing that the doped $Tb^{3+}$ ions do not cause obvious change in crystal phase.

Fig. 2 shows the enlarged XRD patterns near $2\theta$=28° for the (111) peak. It is worth noting that the diffraction peak of $CeF_3$:$Tb^{3+}$ nanocrystals was shifted to larger angles compared with the undoped $CeF_3$ nanodisks (as

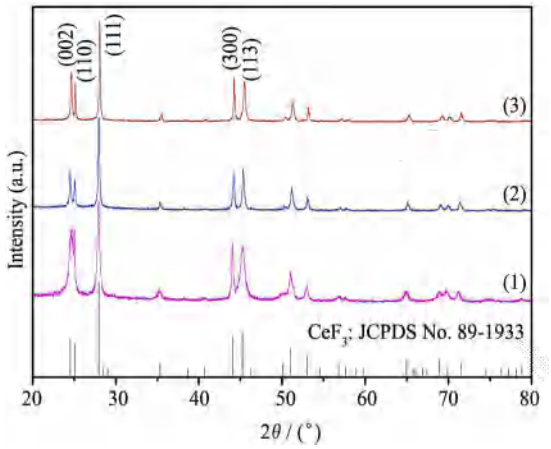


Fig. 1 XRD patterns of $CeF_3$ ultrasonic irradiation for 2 h (1), $CeF_3$:$Tb^{3+}$ stirring for 2 h (2) and $CeF_3$:$Tb^{3+}$ ultrasonic irradiation for 2 h (3) and the literature values of JCPDS No. 89-1933 for bulk $CeF_3$

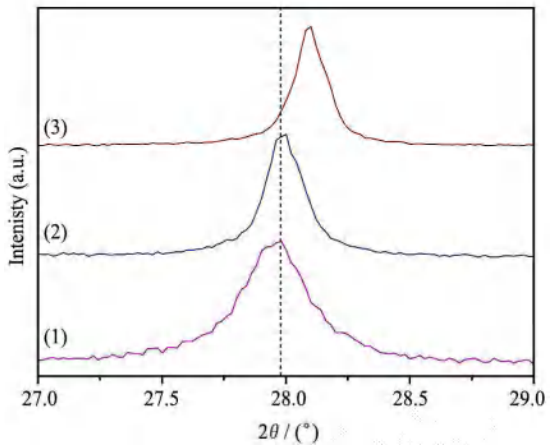


Fig. 2 Enlarged XRD patterns near $2\theta$=28° for the (111) peak

shown in Fig. 2). According to Bragg equation, we could determine that the lattice parameters become smaller, indicating that the large $Ce^{3+}$ ions (radius is 1.034 nm) were substituted by small $Tb^{3+}$ ions (radius is 0.923 nm), so the diffraction peaks move to high angles. In addition, the peak in Fig. 2(3) shifts toward much higher angle as compared to that in Fig. 2(2). That is because the ultrasonic irradiation method can provide an unusual chemical environment, so the $Tb^{3+}$ ions are more easily diffused into the crystal lattice of $CeF_3$. That is to say, more $Tb^{3+}$ ions substitute the sites of $Ce^{3+}$ ion when the samples were prepared by ultrasonic irradiation method.

### 2.2 Morphology

The size and morphology of the samples were characterized by SEM. Fig. 3 shows the SEM images of the as-synthesized samples. Fig. 3(a) and (b) show SEM images of the $CeF_3$:$Tb^{3+}$ prepared with ultrasonic irradiation for 2 h. The SEM image with a low-resolution micrograph (Fig. 3(a)) reveals that the $CeF_3$:$Tb^{3+}$ is entirely comprised of disks with a uniform size and round shape. The high-resolution micrograph (Fig. 3(b)) illustrates that the mean thickness and diameter of the disks are 80 and 450 nm, respectively. The $CeF_3$ sample that was prepared via sonochemical method has the similar morphology with the $CeF_3$:$Tb^{3+}$ sample, as shown in Fig. 3(c) and (d). These results indicated that the doped $Tb^{3+}$ ions have no obvious effect on the morphology of $CeF_3$ nanodisks. That is to say, the $Tb^{3+}$ ions are well-dissolved in the $CeF_3$ nanocrystals, which is in good agreement with the XRD results.

Fig. 3(e–f) are the SEM images of the $CeF_3$:$Tb^{3+}$ synthesized via stirring method with different magnifications, indicating that the product is composed of a large quantity of particles with diameter ranging from 50 to 175 nm. Moreover, high-resolution micrograph (Fig. 3(f)) displays that their shapes are discoid to a certain extent. It can be assumed that the disk-like nanostructures can be obtained via the stirring method if prolonging the reaction time. Additionally, in the case of stirring method, only a little product could be obtained after magnetic stirring for 2 h, indicating that only a little portion of the [BMIM][$BF_4$] was hydrolyzed in the reaction. Based on the above results, it is visible that the ultrasonic irradiation could notably shorten the reaction time, accelerate the hydrolyzation rate of $[BF_4]^-$ ions of [BMIM][$BF_4$], increase the crystallinity and improve product yield.

Fig. 4 displays low and high-resolution TEM images of the $CeF_3$:$Tb^{3+}$ nanodisks. The low-resolution TEM image (Fig. 4(a)) shows that the as-synthesized $CeF_3$:$Tb^{3+}$ crystals are composed of nanodisks with thickness of 60–65 nm and diameter of 260–425 nm. The high-resolution TEM image (Fig. 4(b)) shows the high crystallinity nature of these nanodisks. The distances between two fringes were measured to be 0.32 and 0.35 nm, corresponding to the *d* spacing of the (111) and (110) lattice planes in the $CeF_3$ crystals, respectively. The inset figure in Fig. 4(a) is a SAED pattern of one particle. The SAED pattern indicates that the $CeF_3$:$Tb^{3+}$ nanodisks are single crystal in nature. These results indicate that highly crystalline products can be obtained via the ultrasound assisted ionic liquid method.

### 2.3 Formation mechanism

In the case of the current system, the possible formation mechanism of nanodisks under ultrasound condition

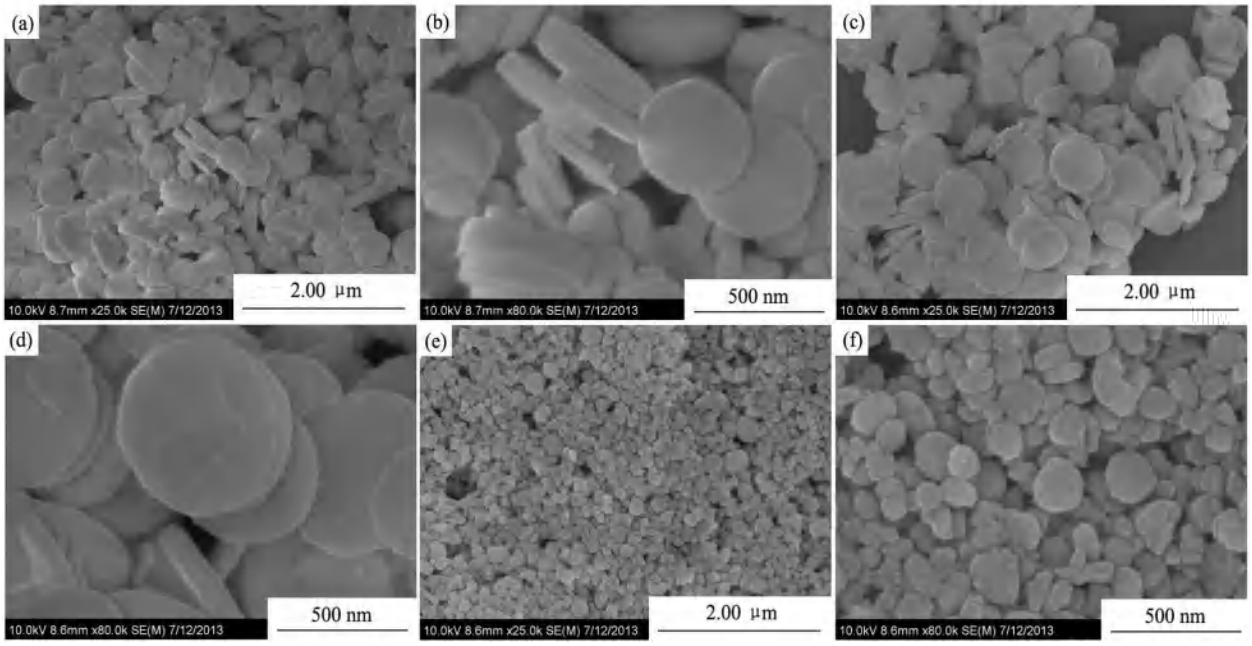


Fig. 3 Low-resolution and high-resolution SEM images of the as-synthesized samples

(a) and (b) $CeF_3$:$Tb^{3+}$ nanodisks with ultrasonic irradiation for 2 h; (c) and (d) $CeF_3$ nanodisks with ultrasonic irradiation for 2 h; (e) and (f) $CeF_3$:$Tb^{3+}$ nanoparticles under stirring for 2 h

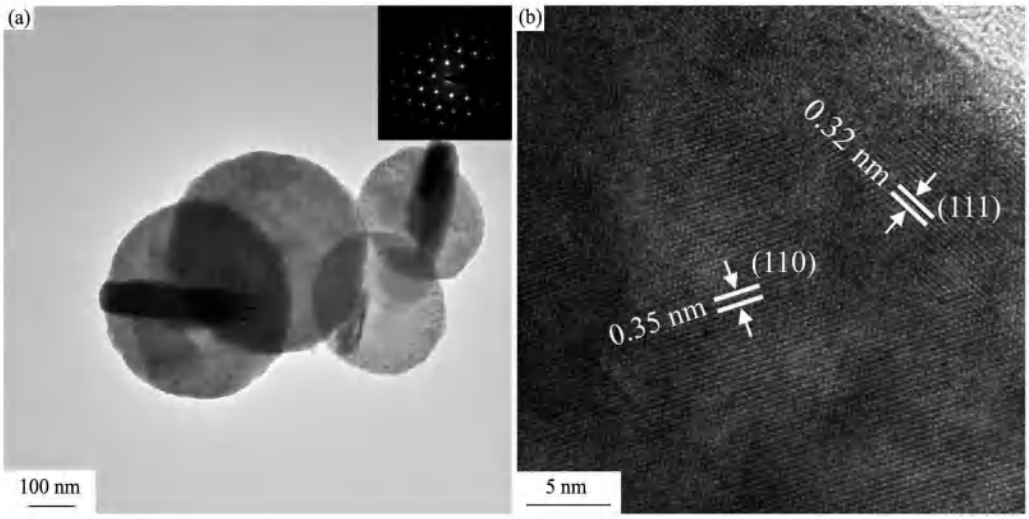


Fig. 4 TEM (a) and HRTEM (b) images of $CeF_3$:$Tb^{3+}$ nanodisks (Inset figure in Fig. 4(a) is the corresponding SAED pattern)

is proposed as follows. When [BMIM][$BF_4$] was slowly added to the $Ln(NO_3)_3$ (Ln=Ce,Tb) aqueous solution, the $[BF_4]^-$ ions of [BMIM][$BF_4$] interacted strongly with water molecules by hydrogen bonds[17]. Then, the mixed homogeneous aqueous solution was irradiated with high-intensity ultrasound. It is observed that many small cavities grew rapidly under the Ti-horn. Once these cavities have overgrown, they could no longer sustain themselves, the surrounding liquid rushed in and these cavities imploded. This phenomenon is the so called acoustic cavitation: the formation, growth, and implosive collapse of bubbles in a liquid, which can generates hot spots with temperatures of roughly 5000 °C, pressures of about 500 atmospheres, and a very short lifetime[18]. The generated transient high temperature and pressure could partly decompose [BMIM][$BF_4$] into $[BMIM]^+$ cations and $[BF_4]^-$ anions, and furthermore the $[BF_4]^-$ anions undergo hydrolysis to produce $F^-$ ions, $BF_3{\cdot}H_2O$, HF and $BO_3^{3-}$[19,20]. Subsequently, the $F^-$ ions would react with $Ln^{3+}$ ions to form tiny $LnF_3$ nuclei, and the formed $LnF_3$ nuclei suspended in solution. And under ultrasonic irradiation condition, the cavitation and shock waves were created which can dramatically accelerate $LnF_3$ nuclei to high velocities, leading to the interparticle collision and effective fusion at the point of collision[21]. Therefore, tiny $LnF_3$ nuclei collide together to form small $LnF_3$ particles. For the hexagonal $LnF_3$ crystals, there is a growth competition between (100) planes and (001) planes. In generally, the growth rate of (100) planes is relatively larger than that of (001) planes[22]. Therefore, the tiny $LnF_3$ particles formed initially grow the primary building blocks with nanodisks shape[23]. Additionally, it is notable that the ILs can self-assemble into disk-like supramolecular structure through the π-π stack interaction of the imidazolium rings at the higher ionic liquid concentrations in aqueous solution[24,25]. The formed supramolecular structure can be used as a soft template to determine the shape and size of the products[26]. Moreover, the decomposed products of IL and $NO_3^-$ anions could also be selectively absorbed on the surface of the (001) planes of these $LnF_3$ nanodisks, which further slowed down the growth rate along the [0001] direction, consequently inhibiting the longitudinal growth along the [0001] direction with a relative enhancement of the growth sideways and gave rise to the 2D disk-like $LnF_3$ nanostructures[11,27].

While the experiment was performed with magnetic stirring, the cavitation and shock waves were absent. As a result, it needed much longer time to decompose the [BMIM][$BF_4$]. In the same reaction time, the chemical species produced by the decomposition of the [BMIM][$BF_4$] were less with respect to that under ultrasonic irradiation. Consequently, the chemical species absorbed on the surface of the (001) planes of the $LnF_3$ particles were less, leading to the decreasing inhibitory degree of the crystal growth along the [0001] direction. Therefore, the $LnF_3$ nanoparticles were formed instead of nanodisks. In a word, both the ultrasound and the [BMIM][$BF_4$] have great effect on the formation of $CeF_3$:$Tb^{3+}$ nanodisks.

### 2.4 Luminescence properties

Fig. 5 shows the excitation (1) and emission (2) spectra of $CeF_3$:$Tb^{3+}$ nanodisks that were obtained by ultrasound irradiation. The excitation spectrum ($\lambda_{em}$=544 nm) (Fig. 5(1)) shows a broad band ranging from 200 to 300 nm, peaking at 254 nm, which can be attributed to the 4f–5d absorption of $Ce^{3+}$ ions[28]. Meanwhile, it can be seen that some weak excitation peaks in 300 to 500 nm region are related to the f–f transitions of $Tb^{3+}$ ions: $^7F_6\rightarrow{}^5D_0$, $^7F_6\rightarrow{}^5L_7$, $^7F_6\rightarrow{}^5L_9$, $^7F_6\rightarrow{}^5G_5$, $^7F_6\rightarrow{}^5G_6$ and $^7F_6\rightarrow{}^5D_4$[29,30]. Fig. 5(2) shows the emission spectra of $CeF_3$:$Tb^{3+}$ ($\lambda_{ex}$=254 nm), the four characteristic emission peaks at 491 nm ($^5D_4\rightarrow{}^7F_6$), 544 nm ($^5D_4\rightarrow{}^7F_5$), 585 nm ($^5D_4\rightarrow{}^7F_4$), and 622 nm ($^5D_4\rightarrow{}^7F_3$) were observed in the emission spectra[31,32]. Amongst these, the $^5D_4\rightarrow{}^7F_5$

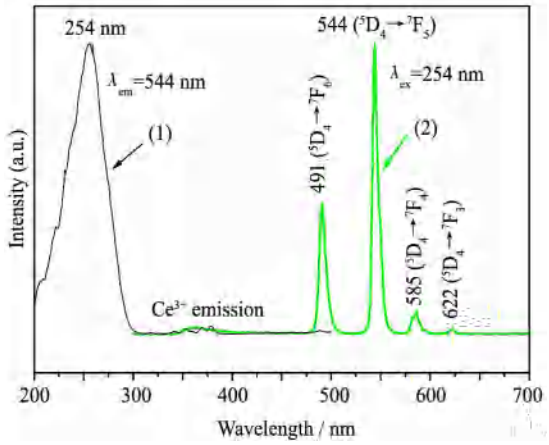


Fig. 5 Excitation (1) and emission (2) spectra of $CeF_3$:$Tb^{3+}$ nanodisks

emission at 544 nm is the strongest. Besides, it can be clearly observed that there is a very weak emission band of $Ce^{3+}$ at 360 nm, indicating that an energy transfer from $Ce^{3+}$ to $Tb^{3+}$ occurs in the $CeF_3$:$Tb^{3+}$ nanodisks. The strong and well defined emission peaks of $CeF_3$:$Tb^{3+}$ nanodisks also show that the $Tb^{3+}$ ions were well dissolved in $CeF_3$ nanocrystals.

Fig. 6 shows the emission spectra of $CeF_3$:$Tb^{3+}$ nanoparticles (1) and nanodisks (2) that were obtained via stirring and ultrasonic irradiation, respectively. Both the samples were measured under identical conditions with the excitation wavelength of 254 nm. Although the two emission spectra are similar in profile with the major peak position at 544 nm, the emission intensity of the $CeF_3$:$Tb^{3+}$ nanodisks is much higher than that of $CeF_3$:$Tb^{3+}$ nanoparticles. Generally, such differences in the PL spectra can be caused by factors like the extent of crystallinity, morphology, size, the content of luminescent ions in phosphors. XRD results revealed that the discoid particles (Fig. 1(3)) and the nanoparticles (Fig. 1(2)) prepared with or without ultrasonic irradiation are highly crystalline with the same crystal structure and similar crystal intensity. Therefore, the difference in the PL intensity may be due to the difference of the morphology, size and the content of $Tb^{3+}$ ions in $CeF_3$:$Tb^{3+}$ phosphors, which have similar phenomenon observed by other researchers[14,33,34]. In addition, it is known that ultrasound irradiation of liquids caused by acoustic cavitation can generate transient high temperature and pressure, which may lead to the fewer surface defects of the nanodisks synthesized via ultrasonic irradiation. In contrast, the nanoparticles synthesized via magnetic stirring possess more surface defects. Some of these defects act as nonradiative recombination centers, and they may be responsible for the decrease in the luminescence intensity. A more extensive investigation of the differences in the luminescent properties of the products with different morphologies, crystal structures, sizes and dimensions will be further investigated in our future work.

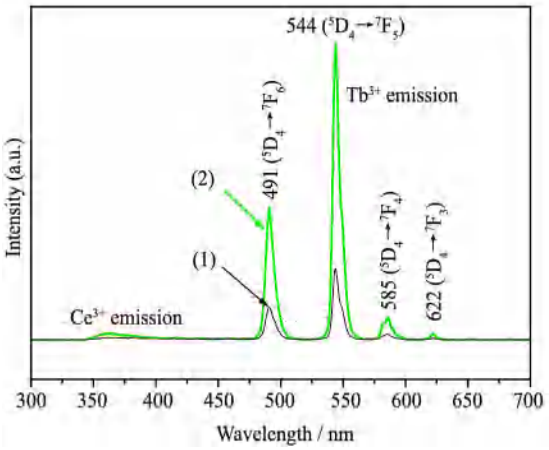


Fig. 6 Emission spectra of $CeF_3$:$Tb^{3+}$ nanoparticles (1) and nanodisks (2)

## 3 Conclusions

In summary, 2D $CeF_3$ and $CeF_3$:$Tb^{3+}$ nanodisks were synthesized by a facile and environmentally friendly ultrasound assisted ionic liquid method. The $CeF_3$:$Tb^{3+}$ nanodisks with average diameter of 450 nm and thickness of 80 nm were obtained with ultrasound and ionic liquid, whereas granular nanoparticles of $CeF_3$:$Tb^{3+}$ were obtained with stirring and ionic liquid. Furthermore, the $CeF_3$:$Tb^{3+}$ nanodisks exhibited a strong green emission from the $^5D_4\rightarrow^7F_J$ ($J$=6,5,4,3) levels under 254 nm UV excitation. The emission spectra of the $CeF_3$:$Tb^{3+}$ samples with different morphologies that prepared by the two methods had similar features, but the emission intensity of the $CeF_3$:$Tb^{3+}$ nanodisks prepared via ultrasound irradiation was higher than that of the granular crystals prepared by stirring.

In this system, [BMIM][$BF_4$] was used as the fluorine source, co-solvent and temple. At the same time, ultrasonic irradiation could accelerate reaction velocity, shortened reaction time, and improved the luminescence intensity. Thus, ultrasound assisted ionic liquid method has a potential application for synthesis of other luminescent materials.

## References:

[1] Stouwdam J W, van Veggel F C J M. Near-infrared emission of redisporsible $Er^{3+}$, $Nd^{3+}$, and $Ho^{3+}$ doped $LaF_3$ nanoparticles. *Nano Lett.*, 2002, **2**(7): 733.

[2] Zhang L S, Li W, Hu X H, Peng Y L, Hu J Q, Kuang X Y, Song L L, Chen Z G. Facile one-pot sonochemical synthesis of hydrophilic ultrasmall $LaF_3$:Ce,Tb nanoparticles with green luminescence. *Prog. Nat. Sci.*, 2012, **22**(5): 488.

[3] Teng X, Zhu Y H, Wei W, Wang S C, Huang J F, Naccache R, Hu W B, Tok A L Y, Han Y, Zhang Q C, Fan Q L, Huang W, Capobianco J A, Huang L. Lanthanide-doped $Na_xScF_{3+x}$ nanocrystals: crystal structure evolution and multicolor tuning. *J. Am. Chem. Soc.*, 2012, **134**(20):

8340.

[4] Wang F, Liu X G. Recent advances in the chemistry of lanthanide-doped upconversion nanocrystals. *Chem. Soc. Rev.*, 2009, **38**(4): 976.

[5] Wang Y F, Liu G Y, Sun L D, Xiao J W, Zhou J C, Yan C H. $Nd^{3+}$-sensitized upconversion nanophosphors: efficient in vivo bioimaging probes with minimized heating effect. *ACS Nano*., 2013, **7**(8): 7200.

[6] Wang X Y, Shan S N, Fei W W, Du L F, Jia N Q. Facile Synthesis of monodisperse, size-controlled hexagonal-phase $NaYF_4$ up-conversion luminescent nanorods. *Integr. Ferroelectr.*, 2012, **138**(1): 123.

[7] Ding Y J, Teng X, Zhu H, Wang L L, Pei W B, Zhu J J, Huang L, Huang W. Orthorhombic $KSc_2F_7$:Yb/Er nanorods: controlled synthesis and strong red upconversion emission. *Nanoscale*, 2013, **5**(23): 11928.

[8] Qiu S Q, Dong J X, Chen G X. Synthesis of $CeF_3$ nanoparticles from water-in-oil microemulsions. *Powder Technol.*, 2000, **113**(1-2): 9.

[9] Moses W W, Derenzo S E. Cerium fluoride, a new fast, heavy scintillator. *Ieee T. Nucl. Sci.*, 1989, **36**(1): 173.

[10] Wang Z L, Quan Z W, Jia P Y, Lin C K, Luo Y, Chen Y, Fang J, Zhou W, O'Connor C J, Lin J. A facile synthesis and photoluminescent properties of redispersible $CeF_3$, $CeF_3$:$Tb^{3+}$, and $CeF_3$:$Tb^{3+}$/$LaF_3$ (core/shell) nanoparticles. *Chem. Mater.*, 2006, **18**(8): 2030.

[11] Li C X, Liu X M, Yang P P, Zhang C M, Lian H Z, Lin J. $LaF_3$, $CeF_3$, $CeF_3$:$Tb^{3+}$, and $CeF_3$:$Tb^{3+}$@$LaF_3$ (core-shell) nanoplates: hydrothermal synthesis and luminescence properties. *J. Phys. Chem. C*, 2008, **112**(8): 2904.

[12] Xu C X, Sun X W, Dong Z L, Cui Y P, Wang B P. Nanostructured single-crystalline twin disks of zinc oxide. *Cryst. Growth Des.*, 2007, **7**(3): 541.

[13] Guo H. Photoluminescent properties of $CeF_3$:$Tb^{3+}$ nanodiskettes prepared by hydrothermal microemulsion. *Appl. Phys. B*, 2006, **84**(1-2): 365.

[14] Zhu L, Li Q, Liu X D, Li J Y, Zhang Y F, Meng J, Cao X Q. Morphological control and luminescent properties of $CeF_3$ nanocrystals. *J. Phys. Chem. C*, 2007, **111**(16): 5898.

[15] Wasserscheid P, Keim W. Ionic liquids–new "solutions" for transition metal catalysis. *Angew. Chem. Int. Ed.*, 2000, **39**(21): 3772.

[16] Sheldon R. Catalytic reactions in ionic liquids. *Chem. Commun.*, 2001, (23): 2399.

[17] Singh T, Kumar A. Aggregation behavior of ionic liquids in aqueous solutions: effect of alkyl chain length, cations, and anions. *J. Phys. Chem. B*, 2007, **111**(27): 7843.

[18] Suslick K S. Sonochemistry. *Science*, 1990, **247**: 1439.

[19] Zhang T, Guo H, Qiao Y M. Facile synthesis, structural and optical characterization of $LnF_3$:Re nanocrystals by ionic liquid-based hydrothermal process. *J. Lumin.*, 2009, **129**(8): 861.

[20] Zhu L, Meng J, Cao X Q. Sonochemical synthesis and luminescence properties of single-crystalline $BaF_2$:$Eu^{3+}$ nanospheres. *J. Solid State Chem.*, 2007, **180**(11): 3101.

[21] Zhu L, Meng J, Cao X Q. Sonochemical synthesis of monodispersed $KY_3F_{10}$:$Eu^{3+}$ nanospheres with bimodal size distribution. *Mater. Lett.*, 2008, **62**(17-18): 3007.

[22] Bao L Y, Li Z Q, Tao Q L, Xie J J, Mei Y Y, Xiong Y J. Controlled synthesis of uniform $LaF_3$ polyhedrons, nanorods and nanoplates using NaOH and ligands. *Nanotechnology*, 2013, **24**(14): 145604.

[23] Li C X, Ma P A, Yang P P, Xu Z H, Li G G, Yang D M, Peng C, Lin J. Fine structural and morphological control of rare earth fluorides $REF_3$ (RE=La–Lu, Y) nano/microcrystals: microwave-assisted ionic liquid synthesis, magnetic and luminescent properties. *CrystEngComm*, 2011, **13**(3): 1003.

[24] Zhou Y, Schattka J H, Antonietti M. Room-temperature ionic liquids as template to monolithic mesoporous silica with wormlike pores via a sol-gel nanocasting technique. *Nano Lett.*, 2004, **4**(3): 477.

[25] Bowers J, Butts C P, Martin P J, Vergara-Gutierrez M C, Heenan R K. Aggregation behavior of aqueous solutions of ionic liquids. *Langmuir*, 2004, **20**(6): 2191.

[26] Kundu S, Kar A, Patra A. Morphology dependent luminescence properties of rare-earth doped lanthanum fluoride hierarchical microstructures. *J. Lumin.*, 2012, **132**(6): 1400.

[27] Zhu L, Meng J, Cao X Q. Facile synthesis and photoluminescence of europium ion doped $LaF_3$ nanodisks. *Eur. J. Inorg. Chem.*, 2007, **2007**(24): 3863.

[28] Boyer J C, Gagnon J, Cuccia L A, Capobianco J A. Synthesis, characterization, and spectroscopy of $NaGdF_4$:$Ce^{3+}$, $Tb^{3+}$/$NaYF_4$ core/shell nanoparticles. *Chem. Mater.*, 2007, **19**(14): 3358.

[29] Kam C H, Buddhudu S. Emission properties of GdOBr: $Ce^{3+}$ and $Tb^{3+}$ phosphors. *Mater. Lett.*, 2002, **54**(5-6): 337.

[30] Yang Y M, Bao A, Lai H, Tao Y C, Yang H. Luminescent properties of $SrAl_2B_2O_7$:$Ce^{3+}$, $Tb^{3+}$. *J. Phys. Chem. Solids*, 2009, **70**(10): 1317.

[31] Qu X S, Yang H K, Pan G H, Chung J W, Moon B K, Choi B C, Jeong J H. Controlled fabrication and shape-dependent luminescence properties of hexagonal $NaCeF_4$, $NaCeF_4$:$Tb^{3+}$ nanorods via polyol-mediated solvothermal route. *Inorg. Chem*., 2011, **50**(8): 3387.

[32] Phaomei G, Singh W R. Effect of solvent on luminescence properties of re-dispersible $LaF_3$:$Ln^{3+}$ ($Ln^{3+}$=$Eu^{3+}$, $Dy^{3+}$, $Sm^{3+}$ and $Tb^{3+}$) nanoparticles. *J. Rare Earths*, 2013, **31**(4): 347.

[33] Yu L X, Liu H, Nogami M. The affects of doping $Eu^{3+}$ on structures and morphology of $ZrO_2$ nanocrystals. *Opt. Mater.*, 2010, **32**(9): 1139.

[34] Freris I, Riello P, Enrichi F, Cristofori D, Benedetti A. Synthesis and optical properties of sub-micron sized rare earth-doped zirconia particles. *Opt. Mater.*, 2011, **33**(11): 1745.